J|A|C|S
ARTICLES
Published on Web 02/24/2007

Tuning the Hydrolytic Aqueous Chemistry of Osmium Arene Complexes with N,O-Chelating Ligands to Achieve Cancer Cell Cytotoxicity

Anna F. A. Peacock, Simon Parsons, and Peter J. Sadler*
Contribution from the School of Chemistry, University of Edinburgh, West Mains Road, Edinburgh EH9 3JJ, U.K.

Received November 21, 2006; E-mail: p.j.sadler@ed.ac.uk

Abstract: Potential biological and medical applications of organometallic complexes are hampered by a lack of knowledge of their aqueous solution chemistry. We show that the hydrolytic and aqueous solution chemistry of half-sandwich Os^{II} arene complexes of the type [(η^6-arene)Os(XY)Cl] can be tuned with XY chelating ligands to achieve cancer cell cytoxicity comparable to carboplatin. Complexes containing arene = *p*-cymene, XY = N,O-chelating ligands glycinate (**1**), L-alaninate (**2**), α-aminobutyrate (**3**), β-alaninate (**4**), picolinate (**5**), or 8-hydroxyquinolinate (**7**) were synthesized. Although, **1**−**4** and **7** hydrolyzed rapidly (<min), complexes with π-acceptor pyridine as N-donor and carboxylate as O-donor (**5** and **6**) hydrolyzed much more slowly ($t_{1/2}$ = 0.20 and 0.52 h, 298 K). The aqua picolinate complexes were more acidic (pK_a^* = 6.67, 6.33) than the other aqua adducts (pK_a^* = 7.17−7.71). At biological test concentrations (micromolar), the chelating ligands dissociated from complexes **1**−**4** to give the inert hydroxo-bridged dinuclear species [(η^6-arene)Os(μ-OH)$_3$Os(η^6-arene)]$^+$ (**8**), and these complexes were inactive toward human lung A549 and ovarian A2780 cancer cells. In contrast, **5**−**7** were cytotoxic, especially **6** (IC_{50} values of 8 and 4.2 μM). The X-ray structures of 9-ethylguanine, [(η^6-*p*-cym)Os(pico)(9EtG-*N7*)]PF_6, and 9-ethyladenine, [(η^6-*p*-cym)-Os(pico)(9EtA-*N7*)]PF_6, adducts of **5** are reported (the first reported for G or A adducts of Os^{II}). Crystals of the 9EtA complex contain homoadenine base pairing. The 9EtG adduct in particular exhibits remarkable aqueous kinetic stability. This work shows how the rational control of chemical reactivity (hydrolysis, acidity, formation of hydroxo-bridged dinuclear species) can allow the design of cytotoxic anticancer Os^{II} arene complexes.

Introduction

Transition metal complexes offer enormous scope for the design of therapeutic agents with novel mechanisms of action.[1] Advances in this field depend upon demonstrations that the concept of rational design can be applied to metal complexes. For this, knowledge of how to control the thermodynamics and kinetics of ligand substitution and redox reactions under biologically relevant conditions is essential, in particular, the hydrolytic chemistry. This is well illustrated for the platinum anticancer field. It was apparent early on[2] that an understanding of the aqueous chemistry of cisplatin and related complexes, including aquation rates, hydrolysis equilibria, acidity of aqua adducts, formation of hydroxo-bridged oligomers, aids not only the design of new generations of platinum agents but also an understanding of the mechanism of cytotoxicity. The early use of cisplatin, which hydrolyzes readily, has been supplemented by more stable complexes such as carboplatin and oxaliplatin which have less side effects.[3] Recently, the design of active trans diam(m)ine Pt^{II} complexes has been aided by the discovery that trans carboxylato ligands can decrease kinetic activity by about an order of magnitude compared to their chloro analogues.[4] The choice of the types of coordinated ligands and coordination geometry provides an ability to "fine-tune" the chemical reactivity of complexes, potentially allowing control of pharmacological properties, including cell uptake, distribution, DNA binding, metabolism, and toxic side effects.

Organometallic chemistry offers a potentially rich field for biological and medical applications,[5] but, as pointed out recently,[6] a lack of understanding of the aqueous chemistry of organometallic complexes is currently a major obstacle for further developments. This is particularly true for osmium(II) arene complexes.[7−9] Here we attempt to design active osmium half-sandwich complexes by controlling their aqueous chemistry.

(1) (a) Guo, Z.; Sadler, P. J. *Adv. Inorg. Chem.* **2000**, *49*, 183−306. (b) Yan, Y. K.; Melchart, M.; Habtemariam, A.; Sadler, P. J. *Chem. Commun.* **2005**, *38*, 4764−4776. (c) Melchart, M.; Sadler, P. J. In *Bioorganometallics*; Jaouen, G., Ed.; Wiley-VCH: Paris, 2005; Vol. 1, pp 39−64. (d) Allardyce, C. S.; Dorcier, A.; Scolaro, C.; Dyson, P. J. *Appl. Organomet. Chem.* **2005**, *19*, 1−10.
(2) (a) Howe-Grant, M. E.; Lippard, S. J. *Metal Ions Biol. Syst.* **1980**, *11*, 63−196. (b) Martin, R. B. *ACS Symp. Ser.* **1983**, *209*, 231−244.
(3) Reedijk J. *Chem. Commun.* **1996**, 801−806.
(4) Bulluss, G. H.; Knott, K. M.; Ma, E. S. F.; Aris, S. M.; Alvarado, E.; Farrell, N. *Inorg. Chem.* **2006**, *45*, 5733−5735.
(5) (a) Halpern, J. *Pure Appl. Chem.* **2001**, *73*, 209−220. (b) Fish, R. H.; Jaouen, G. *Organometallics* **2003**, *22*, 2166−2177.
(6) Jaouen, G.; Beck, W.; McGlinchey, M. J. In *Bioorganometallics: Biomolecules, Labeling, Medicine*; Jaouen, G., Ed.; Wiley-VCH: Weinheim, Germany, 2006; pp 1−37.
(7) Hung, Y.; Kung, W.; Taube, H. *Inorg. Chem.* **1981**, *20*, 457−463.
(8) Stebler-Röthlisberger, M.; Hummel, W.; Pittet, P. A.; Bürgi, H. B.; Ludi, A.; Merbach, A. E. *Inorg. Chem.* **1988**, *27*, 1358−1363.
(9) Mui, H. D.; Brumaghim, J. L.; Gross, C. L.; Girolami, G. S. *Organometallics* **1999**, *18*, 3264−3272.

10.1021/ja068335p CCC: $37.00

Osmium complexes are usually considered to be relatively inert in keeping with the normal behavior of a third row transition metal. However, our recent work on ruthenium arene complexes has shown that aqueous reactivity of $[(\eta^6\text{-arene})Ru(XY)Z]^{n+}$ complexes is highly dependent on the nature of the chelating ligand XY and monodentate ligand Z (the leaving group), as well as the arene.[10,11] A similar pattern of reactivity may therefore apply to osmium, the heavier congener of ruthenium. A theoretical analogy between cisplatin and Ru^{II} arene anticancer complexes has recently been proposed by Deubel et al.[12]

Here we investigate the tuning of the reactivity of osmium(II) arene complexes $[(\eta^6\text{-arene})Os(XY)Cl]$ containing XY = an anionic N,O-chelating ligand with a primary amine or pyridine as the N-donor and carboxylate or aryloxide as the O-donor. We have studied the rate of hydrolysis, acidity of the aqua adducts, dynamic chelate ring opening, interactions with nucleobases, and relationship to cancer cell cytotoxicity. Our data suggest that the aqueous solution chemistry of organometallic osmium arene complexes can be controlled for the rational design of biologically active agents.

Experimental Section

Materials. $OsCl_3 \cdot nH_2O$ was purchased from Alfa Aesar, sodium methoxide, α-aminoisobutyric acid, 2-picolinic acid, silver hexafluorophosphate, 9-ethylguanine, 9-ethyladenine, adenosine, cytidine, and thymidine were from Sigma, and sodium glycinate, L-alanine, β-alanine, 8-hydroxyquinoline, and deuterated solvents were from Aldrich. The dimers $[(\eta^6\text{-}p\text{-cym})OsCl_2]_2$ and $[(\eta^6\text{-bip})OsCl_2]_2$ were prepared by previously reported procedures.[13,14] Methanol was distilled over magnesium/iodine prior to use.

Complexes **1**−**7** were synthesized from the dimeric precursor $[(\eta^6\text{-arene})OsCl_2]_2$, using procedures similar to those reported previously for other half-sandwich Ru^{II} arene complexes.[15,16]

Preparation of Complexes: [(η⁶-*p*-cym)Os(gly)Cl] (1). A solution of sodium glycinate (12.3 mg, 0.13 mmol) and $[(\eta^6\text{-}p\text{-cym})OsCl_2]_2$ (47.3 mg, 0.06 mmol) in MeOH (5 mL) was stirred at ambient temperature for 5.5 h, the solvent removed on a rotary evaporator, and the residue extracted with dichloromethane and filtered through a cotton wool plug. The solvent volume was reduced to ca. 3 mL, and the solution stored at 253 K overnight. The pale yellow powder which formed was recovered by filtration, washed with diethyl ether (10 mL), and air-dried. Yield: 33.1 mg (59%). Anal. Calcd for **1**+H_2O $C_{12}ClH_{20}NO_3Os$ (451.98): C, 31.89; H, 4.46; N, 3.10%. Found: C, 31.98; H, 3.92; N, 3.05%. ^{1}H NMR (MeOD-d_4): δ = 6.02 (d, 1H, J = 5.3 Hz), 5.98 (d, 1H, J = 5.3 Hz), 5.80 (d, 1H, J = 5.3 Hz), 5.76 (d, 1H, J = 5.3 Hz), 3.20 (m, 2H), 2.73 (sept, 1H, J = 6.8 Hz), 2.25 (s, 3H), 1.32 (d, 6H, J = 7.0 Hz).

[(η⁶-*p*-cym)Os(L-ala)Cl] (2). A solution of L-alanine (11.6 mg, 0.13 mmol), sodium methoxide (7.7 mg, 0.14 mmol), and $[(\eta^6\text{-}p\text{-cym})OsCl_2]_2$ (47.2 mg, 0.06 mmol) in MeOH (5 mL) was stirred at ambient temperature for 22 h. The solvent was removed on a rotary evaporator, and the residue extracted with dichloromethane and filtered through a cotton wool plug. The solvent was again removed and the product recovered by titrating with diethyl ether. Yield: 46 mg (86%). Anal. Calcd for $C_{13}ClH_{20}NO_2Os$ (447.99): C, 34.85; H, 4.50; N, 3.13%. Found: C, 34.38; H, 4.01; N, 3.00%. ^{1}H NMR (MeOD-d_4): δ = 7.51 (br, NH), 6.40 (br, NH), 6.02 (d, 2H), 5.99 (d, 1H), 5.95 (d, 1H), 5.81 (m, 3H), 5.74 (d, 1H), 5.29 (br, NH), 3.98 (br, NH), 3.40 (q, 1H), 3.25 (q, 1H), 2.73 (sept, H), 2.72 (sept, H), 2.23 (s, 3H), 2.22 (s, 3H), 1.42 (d, 3H), 1.34 (d, 3H), 1.32 (d, 6H), 1.31 (d, 6H). Diastereoisomers were present in a 1.5:1 ratio.

[(η⁶-*p*-cym)Os(aiba)Cl] (3). A solution of α-aminoisobutyric acid (13.9 mg, 0.13 mmol), sodium methoxide (7.3 mg, 0.14 mmol), and $[(\eta^6\text{-}p\text{-cym})OsCl_2]_2$ (50.8 mg, 0.06 mmol) in MeOH (5 mL) was stirred at ambient temperature for 22 h and filtered through a glass wool plug. The solvent was removed on a rotary evaporator, and the residue extracted with dichloromethane (15 mL) and filtered through a cotton wool plug. The solvent volume was reduced to ca. 3 mL, and the product precipitated after addition of diethyl ether and storage at 253 K for 1 h. The mustard yellow powder was recovered by filtration, washed with diethyl ether (10 mL), and air-dried. Yield: 24.8 mg (42%). Anal. Calcd for $C_{14}ClH_{22}NO_2Os$ (462.01): C, 36.40; H, 4.80; N, 3.03%. Found: C, 36.44; H, 4.68; N, 2.88%. ^{1}H NMR (MeOD-d_4): δ = 6.04 (d, 1H, J = 5.3 Hz), 5.99 (d, 1H, J = 5.0 Hz), 5.87 (d, 1H, J = 5.3 Hz), 5.84 (d, 1H, J = 5.3 Hz), 2.72 (sept, 1H, J = 7.0 Hz), 2.21 (s, 3H), 1.43 (s, 3H), 1.34 (s, 3H), 1.33 (d, 3H, J = 6.9 Hz), 1.30 (d, 3H, J = 6.8 Hz).

[(η⁶-*p*-cym)Os(β-ala)Cl] (4). A solution of β-alanine (12.0 mg, 0.13 mmol), sodium methoxide (7.3 mg, 0.14 mmol), and $[(\eta^6\text{-}p\text{-cym})OsCl_2]_2$ (50.7 mg, 0.06 mmol) in MeOH (4 mL) was stirred at ambient temperature for 19 h. The solvent volume was reduced to ca. 3 mL, and the product precipitated after addition of diethyl ether and storage at 253 K overnight. The yellow powder was recovered by filtration, washed with diethyl ether (10 mL), and air-dried. Yield: 15.1 mg (26.3%). Anal. Calcd for (**4**·H_2O) $C_{13}ClH_{22}NO_3Os$ (466.00): C, 33.51; H, 4.76; N, 3.01%. Found: C, 33.86; H, 4.33: N, 3.06%. ^{1}H NMR (MeOD-d_4): δ = 7.13 (b, 1H), 6.04 (d, 1H, J = 5.3 Hz), 5.96 (d, 1H, J = 5.3 Hz), 5.86 (d, 1H, J = 5.3 Hz), 5.72 (d, 1H, J = 5.3 Hz), 4.14 (b, 1H), 3.04 (m, 1H), 2.75 (sept, 1H, J = 6.8 Hz), 2.64 (m, 1H), 2.46 (ddd, 1H, J = 17.1, 11.1, and 2.7 Hz), 2.29 (dd, 1H, J = 17.0 and 6.3 Hz), 2.19 (s, 3H), 1.31 (d, 3H, J = 6.9 Hz), 1.30 (d, 3H, J = 7.2 Hz).

[(η⁶-*p*-cym)Os(pico)Cl] (5). A solution of picolinic acid (18.6 mg, 0.15 mmol) and sodium methoxide (8.3 mg, 0.15 mmol) in MeOH (3 mL) was stirred at ambient temperature for 45 min and added to a solution of $[(\eta^6\text{-}p\text{-cym})OsCl_2]_2$ (50.8 mg, 0.06 mmol) in MeOH (5 mL) under argon. The resulting mixture was stirred at ambient temperature under argon for 20 h, the solvent was removed on a rotary evaporator, and the residue extracted with dichloromethane and filtered through a cotton wool plug. The solvent volume was reduced to ca. 3 mL, and the product precipitated after addition of diethyl ether. The yellow powder was recovered by filtration, washed with diethyl ether (10 mL), and air-dried. Yield: 55.8 mg (90%). Anal. Calcd for $C_{16}ClH_{18}NO_2Os$ (482.00): C, 39.87; H, 3.76; N, 2.91%. Found: C, 39.87; H, 3.67; N, 2.80%. ^{1}H NMR ($CDCl_3$): δ = 8.78 (d, 1H, J = 5.7 Hz), 8.12 (d, 1H, J = 7.6 Hz), 7.93 (td, 1H, J = 7.6 Hz), 7.50 (td, 1H, J = 6.4 Hz), 5.94 (d, 1H, J = 5.7 Hz), 5.89 (d, 1H, J = 5.7 Hz), 5.72 (d, 1H, J = 5.7 Hz), 5.67 (d, 1H, J = 5.7 Hz), 2.74 (sept, 1H, J = 6.8 Hz), 2.35 (s, 3H), 1.22 (d, 3H, J = 5.3 Hz), 1.21 (d, 3H, J = 5.3 Hz). Crystals of **5** suitable for X-ray diffraction were obtained by evaporation of a chloroform/diethyl ether solution at ambient temperature in the dark.

[(η⁶-bip)Os(pico)Cl] (6). A solution of $[(\eta^6\text{-bip})OsCl_2]_2$ (51.3 mg, 0.06 mmol) in MeOH (5 mL) was refluxed under argon for 1 h before adding a solution of picolinic acid (16.8 mg, 0.14 mmol) and sodium methoxide (7.3 mg, 0.14 mmol) in MeOH (2 mL), which had been stirred at ambient temperature for 30 min. The resulting mixture was stirred at ambient temperature for 20 h, filtered through a cotton wool plug, and the solvent removed on a rotary evaporator. The residue was extracted with dichloromethane, filtered, and the solvent removed again. The resulting solid was redissolved in methanol and the solvent volume reduced until a precipitate began to form. The vessel was stored at

(10) Wang, F.; Chen, H.; Parsons, S.; Oswald, I. D. H.; Davidson, J. E.; Sadler, P. J. *Chem.—Eur. J.* **2003**, *9*, 5810−5820.
(11) Chen, H.; Parkinson, J. A.; Novakova, O.; Bella, J.; Wang, F.; Dawson, A.; Gould, R.; Parsons, S.; Brabec, V.; Sadler, P. J. *Proc. Natl. Acad. Sci. U.S.A.* **2003**, *100*, 14623−14628.
(12) Deubel, D. V.; Lau, J. K.-C. *Chem. Commun.* **2006**, 2451−2453.
(13) Stahl, S.; Werner, H. *Organometallics* **1990**, *9*, 1876−1881.
(14) Peacock, A. F. A.; Habtemariam, A.; Fernández, R.; Walland, V.; Fabbiani, F. P. A.; Parsons, S.; Aird, R. E.; Jodrell, D. I.; Sadler, P. J. *J. Am. Chem. Soc.* **2006**, *128*, 1739−1748.
(15) Carter, L.; Davies, D. L.; Fawcett, J.; Russell, D. R. *Polyhedron* **1993**, *12*, 1599−1602.
(16) Gemel, C.; John, R.; Slugovc, C.; Mereiter, K.; Schmid, R.; Kirchner, K. *J. Chem. Soc., Dalton Trans.* **2000**, 2607−2612.

278 K, and the yellow powder was recovered by filtration, washed with diethyl ether (10 mL), and air-dried. Yield: 23.9 mg (39%). Anal. Calcd for **6**+H_2O $C_{18}ClH_{16}NO_3Os$ (520.01): C, 41.57; H, 3.10; N, 2.69%. Found: C, 41.85; H, 2.50; N, 3.17%. ^{1}H NMR ($CDCl_3$): δ = 8.30 (d, 1H, J = 5.4 Hz), 8.12 (d, 1H, J = 7.9 Hz), 7.86 (t, 1H, J = 7.7 Hz), 7.51 (m, 2H), 7.40 (m, 2H), 7.28 (7, 1H, J = 6.6 Hz), 6.40 (d, 1H, J = 5.3 Hz), 6.36 (d, 1H, J = 4.9 Hz), 6.23 (t, 1H, J = 5.0 Hz), 6.21 (t, 1H, J = 5.0 Hz), 6.15 (t, 1H, J = 5.0 Hz).

[(η^6-*p*-cym)Os(oxine)Cl] (7). A solution of 8-hydroxyquinoline (18.6 mg, 0.13 mmol) and sodium methoxide (6.9 mg, 0.13 mmol) in MeOH (2 mL) was added to a solution of [(η^6-*p*-cym)$OsCl_2$]$_2$ (48.3 mg, 0.06 mmol) in MeOH (4 mL), and the resulting mixture was stirred at ambient temperature for 5 h. The solvent was removed on a rotary evaporator, the residue extracted with acetone (ca. 10 mL), and the solvent volume reduced until a yellow precipitate started to form, and was stored at 253 K overnight. The yellow microcrystalline solid was recovered by filtration, washed with diethyl ether (5 mL), and air-dried. Yield: 43.5 mg (71%). Anal. Calcd for $C_{19}ClH_{20}NOOs$ (504.05): C, 45.27; H, 4.00; N, 2.78%. Found: C, 45.35; H, 4.03; N, 2.68%. ^{1}H NMR ($CDCl_3$): δ = 8.77 (d, 1H, J = 4.9 Hz), 8.05 (d, 1H, J = 8.3 Hz), 7.37 (t, 1H, J = 7.9 Hz), 7.28 (dd, 1H, J = 8.3 and 5.0 Hz), 7.03 (d, 1H, J = 7.9 Hz), 6.84 (d, 1H, J = 7.9 Hz), 5.93 (d, 1H, J = 5.3 Hz), 5.82 (d, 1H, J = 5.3 Hz), 5.70 (d, 1H, J = 5.3 Hz), 5.63 (d, 1H, J = 5.3 Hz), 2.62 (sept, 1H, J = 6.8 Hz), 2.36 (s, 3H), 1.12 (dd, 6H, J = 8.9 and 7.6 Hz). Crystals of **7** suitable for X-ray diffraction were obtained by evaporation of an acetone/diethyl ether solution at ambient temperature in the dark.

[(η^6-*p*-cym)Os(pico)(9EtG)]PF_6 (9PF_6). A solution of [(η^6-*p*-cym)-Os(pico)Cl] (32.6 mg, 0.07 mmol) and $AgPF_6$ (18.5 mg, 1.1 molar equiv) in MeOH (3 mL) was stirred at ambient temperature for 5.5 h. The AgCl precipitate was removed by filtration through a glass wool plug, and 9-ethylguanine (12.2 mg, 1.1 molar equiv) was added to the resulting solution. The reaction mixture was stirred at ambient temperature under argon for ca. 42 h. The resulting pale yellow precipitate was recovered by filtration, washed with methanol (3 mL) and diethyl ether (10 mL), and air-dried. Yield: 28.0 mg (54%). Anal. Calcd for $C_{23}H_{27}N_6O_3OsPF_6$ (770.69): C, 35.84; H, 3.53; N, 10.90%. Found: C, 35.74; H, 3.21; N, 11.23%. ^{1}H NMR (MeOD-d_4): δ = 9.64 (d, 1H, J = 5.3 Hz), 8.12 (td, 1H, J = 7.8 and 1.3 Hz), 7.95 (d, 1H, J = 7.9 Hz), 7.85 (s, 1H), 7.74 (td, 1H, J = 6.8 and 1.5 Hz), 6.50 (d, 1H, J = 5.7 Hz), 6.24 (d, 1H, J = 5.7 Hz), 6.12 (d, 1H, J = 5.7 Hz), 6.04 (d, 1H, J = 5.7 Hz), 4.13 (dq, 2H, J = 7.3 and 2.6 Hz), 2.53 (sept, 1H, J = 6.8 Hz), 2.04 (s, 3H), 1.39 (t, 3H, J = 7.2 Hz), 1.17 (d, 3H, J = 6.8 Hz), 1.03 (d, 3H, J = 6.8 Hz). Crystals of **9PF_6** suitable for X-ray diffraction were obtained by diffusion of diethyl ether into a methanol solution at 278 K.

[(η^6-*p*-cym)Os(pico)(9EtA)]PF_6 (11PF_6). A solution of [(η^6-*p*-cym)-Os(pico)Cl] (24.9 mg, 0.05 mmol) and $AgPF_6$ (13.3 mg, 1.0 molar equiv) in MeOH (3 mL) was stirred at ambient temperature for 2 h. The AgCl precipitate was removed by filtration through a glass wool plug, and 9-ethyladenine (8.6 mg, 1.0 molar equiv) was added. The reaction mixture was stirred at ambient temperature under argon for ca. 78 h. A yellow product precipitated out after addition of diethyl ether and was recovered by filtration, washed with methanol (2 mL) and diethyl ether (10 mL), and air-dried. Yield: 13.3 mg (34%). Anal. Calcd for $C_{23}H_{27}N_6O_2OsPF_6$ (754.69): C, 36.60; H, 3.61; N, 11.14%. Found: C, 37.04; H, 3.57; N, 10.95%. ^{1}H NMR (MeOD-d_4): δ = 9.59 (d, 1H, J = 5.3 Hz), 8.34 (s, 1H), 8.30 (s, 1H), 8.30 (overlapped t, 1H, J = ca. 7 Hz), 8.06 (d, 1H, J = 7.5 Hz), 8.01 (t, 1H, J = 6.3 Hz), 6.64 (d, 1H, J = 5.6 Hz), 6.52 (d, 1H, J = 5.4 Hz), 6.16 (d, 1H, J = 5.3 Hz), 6.11 (d, 1H, J = 5.6 Hz), 4.63 (br s, 2H), 4.31 (sept, 2H, J = 7.0 Hz), 4.25 (sept, 2H, J = 7.0 Hz), 2.64 (sept, 1H, J = 6.8 Hz), 1.85 (s, 3H), 1.41 (t, 3H, J = 7.3 Hz), 1.17 (d, 3H, J = 6.8 Hz), 1.01 (d, 3H, J = 7.0 Hz). Crystals of **11PF_6**·0.5Et_2O suitable for X-ray diffraction were obtained by diffusion of diethyl ether into a methanol solution at 278 K.

Methods and Instrumentation: X-ray Crystallography. All diffraction data were collected using a Bruker (Siemens) Smart Apex CCD diffractometer equipped with an Oxford Cryosystems low-temperature device operating at 150 K. Absorption corrections for all data sets were performed with the multiscan procedure SADABS;[17] structures were solved using either Patterson or direct methods (SHELXL[18] or DIRDIF[19]); complexes were refined against F^2 using SHELXTL, and H-atoms were placed in geometrically calculated positions. The modeling program Diamond 3.0[20] was used for production of graphics. X-ray crystallographic data for complexes **5**, **7**, **9PF_6**, and **11PF_6**·0.5Et_2O are available as Supporting Information and have been deposited in the Cambridge Crystallographic Data Centre under the accession numbers CCDC 626657, 626658, 626655, and 626656, respectively.

NMR Spectroscopy. ^{1}H NMR spectra were acquired on a Bruker AVA 600 (^{1}H = 600 MHz) spectrometer and for D_2O solutions with water suppression by Shaka[21] or presaturation methods. ^{1}H NMR chemical shifts were internally referenced to 1,4-dioxane (3.75 ppm) for aqueous solutions, C*H*D_2OD (3.34 ppm) for methanol-d_4, and C*H*Cl_3 (7.26 ppm) for chloroform-d_1 solutions. All data processing was carried out using XWIN-NMR version 3.6 (Bruker U.K. Ltd.).

Mass Spectrometry. Electrospray ionization mass spectra (ESI-MS) were obtained on a Micromass Platform II mass spectrometer, and D_2O/H_2O solutions were infused directly. The capillary voltage was 3.5 V, and the cone voltage was varied between 20 and 45 V depending on sensitivity. The source temperature was 353 K. Mass spectra were recorded with a scan range of m/z 300−1000 for positive ions.

pH* Measurement. pH* values (pH meter reading without correction for effects of D on glass electrode) of NMR samples in D_2O were measured at ca. 298 K directly in the NMR tube, before and after recording NMR spectra, using a Corning 240 pH meter equipped with a micro combination electrode calibrated with Aldrich buffer solutions at pH 4, 7, and 10.

Hydrolysis. Solutions of **1**−**7** (2 mM) in 5% MeOD-d_4/95% D_2O (v/v) were prepared by dissolution of the complex in MeOD-d_4 followed by rapid dilution with D_2O. Solutions of 50 μM were prepared by subsequent dilution of these 2 mM stock solutions with D_2O (final ratio 0.125% MeOD-d_4/99.875% D_2O (v/v)). The ^{1}H NMR spectra for the 2 mM and 50 μM solutions were recorded within the first 10 min of sample preparation and after incubation at 310 K for 24 h. The speciation of **1**−**7** in 100 mM NaCl was investigated by adding 2.5 M NaCl (25 μL) to the 2 mM NMR sample in D_2O. The effects of varying concentrations of chloride were investigated by preparing aqueous solutions of **5** (1 mM and 50 μM) in 100, 22.7, and 4 mM NaCl in D_2O, recording ^{1}H NMR spectra within the first 10 min of sample preparation, and after incubation at 310 K for 24 h.

The longer term stability of complex **5** was investigated by preparing 1 mM solutions in 5% MeOD-d_4/95% isotonic saline solution (150 mM NaCl) (v/v) by dissolution of **5** in MeOD-d_4 followed by rapid dilution with the isotonic saline solution. ^{1}H NMR spectra were recorded after various time intervals (10 min, 1 week, 2 weeks, and 2 months) during which time the sample was stored at ambient temperature in the dark.

Determination of pK_a* Values. For determinations of pK_a* values (pK_a values for solutions in D_2O), the pH* values of the aqua complexes of **1**−**7** in D_2O (formed in situ by dissolution of the parent chloro complexes) were varied from ca. pH* 3 to 10 by the addition of dilute NaOD and HNO_3, and ^{1}H NMR spectra were recorded. pH* titrations of complexes **9** and **11** were carried out from pH* 3−12 and 1−8,

(17) Sheldrick, G. M. *SADABS*; University of Göttingen: Göttingen, Germany, 2001−2004.
(18) Sheldrick, G. M. *SHELXL-97*, Program for the refinement of crystal structures; University of Göttingen: Göttingen, Germany, 1997.
(19) Beurskens, P. T.; Beurskens, G.; Bosman, W. P.; de Gelder, R.; Garcia-Granda, S.; Gould, R. O.; Israel, R.; Smits, J. M. M. *DIRDIF*; Crystallography Laboratory, University of Nijmegen: The Netherlands, 1996.
(20) Brandenburg, K.; Putz, H. *Diamond. Crystal and Molecular Structure Visualization Crystal Impact GbR*; Bonn, Germany.
(21) Hwang, T. L.; Shaka, A. J. *J. Magn. Reson., Ser. A* **1995**, *112*, 275−279.

respectively. The chemical shifts of the arene ring (**1**−**7**), purine H8 (**9** and **11**), and H2 (**11**) protons were plotted against pH*. The pH* titration curves were fitted to the Henderson−Hasselbalch equation, with the assumption that the observed chemical shifts are weighted averages according to the populations of the protonated and deprotonated species. The experimental and fitting errors in pK_a* values are estimated to be ca. ±0.04 units. These pK_a* values can be converted to pK_a values by use of the equation pK_a = 0.929pK_a* + 0.42 as suggested by Krezel and Bal,[22] for comparison with related values in the literature.

Kinetics for Hydrolysis. Although complexes **1**−**4** and **7** hydrolyzed too rapidly to monitor by ^{1}H NMR, the kinetics for **5** and **6** could be followed at various temperatures (278−298 K). For this, the complex was dissolved in methanol-d_4, and aliquots were added to D_2O (equilibrated at the required temperature) to give a final concentration of ca. 0.8 mM complex in 95% D_2O/5% methanol-d_4 (pH* ca. 3, so that the aqua ligand is not deprotonated). Samples were filtered and spectra recorded at various time intervals. Data, based on peak integrals, were fitted to the appropriate equation for first-order kinetics. The Arrhenius activation energies (E_a), activation enthalpies ($\Delta H^{\ddagger}$), and activation entropies ($\Delta S^{\ddagger}$) were determined from Arrhenius and Eyring plots.[23]

Variable Temperature NMR. The ^{1}H NMR spectra of complexes **4**, **5**, and **7** in D_2O (1 mM, 5% MeOD-d_4 to assist dissolution) were recorded after equilibration at various temperatures. Kinetic data were obtained using the equations $k_c = (\pi\Delta\upsilon)/\sqrt{2}$, where k_c is the rate constant at coalescence, $t_c = 1/k_c$, where t_c is the lifetime of separate isomers at coalescence, and $\Delta G^{\ddagger} = 19.143T_c(10.318 - \log k_c/T_c)$, where T_c is the temperature of coalescence.[24] Similarly, 10 mM solutions of **5** and **7** in methanol-d_4 were recorded after equilibration at various temperatures.

Cancer Cell Cytotoxicity. After plating, human ovarian A2780 cancer cells were treated with Os^{II} complexes on day 3, and human lung A549 cancer cells on day 2, at concentrations ranging from 0.1 to 100 μM. Solutions of the Os^{II} complexes were made up in 0.125% DMSO to assist dissolution. Cells were exposed to the complexes for 24 h, washed, supplied with fresh medium, allowed to grow for three doubling times (72 h), and then the protein content measured (proportional to cell survival) using the sulforhodamine B (SRB) assay.[25] The standard errors are based on three replicates.

Interactions with Nucleobases. The reaction of **5** with nucleobases typically involved addition of a solution containing 1 molar equiv of nucleobase in D_2O (or 1 molar equiv of 9-ethylguanine and 1 molar equiv 9-ethyladenine in a competition reaction), to an equilibrium solution of **5** in D_2O (>90% aqua). The pH* value of the sample was adjusted if necessary so as to remain close to 7.4 (physiological). ^{1}H NMR spectra of these solutions were recorded at 298 K after various time intervals.

NMR spectra of aqueous solutions (D_2O) of the 9EtG and 9EtA complexes **9** and **11**, respectively, were recorded at various concentrations (20 μM to 2 mM) at 298 K and after incubation at 310 K for various time intervals. The equilibrium constant for dissociation of 9EtA from **11** was obtained from the slope of the plot of [bound complex]/[free 9EtA] versus [**5A**], using concentrations based on ^{1}H NMR peak integrals.

Results

Synthesis and Characterization of Complexes. We synthesized seven new Os^{II} arene complexes containing amino acidates, picolinate, or 8-hydroxyquinolinate as anionic N,O-chelating ligands (Figure 1) in good yields via the Cl-bridged dimer, $[(\eta^6\text{-arene})OsCl_2]_2$, arene = *p*-cymene (*p*-cym, **1**−**5**, **7**) or biphenyl (bip, **6**). We determined the X-ray crystal structures of $[(\eta^6\text{-}p\text{-cym})Os(pico)Cl]$ **5** and $[(\eta^6\text{-}p\text{-cym})Os(oxine)Cl]$ **7** (Figure 2). The complexes adopt the familiar pseudo-octahedral "three-leg piano stool" geometry with the osmium π-bonded to the arene ligand (Os ring centroid distances of 1.652(2) Å for **5** and 1.6557(12) Å for **7**), σ-bonded to a chloride (2.4048(13) and 2.4235(7) Å), a pyridine nitrogen (2.090(4) and 2.098(2) Å), and a deprotonated oxygen atom (2.080(3) and 2.081(2) Å) of the chelating ligand, which constitute the three legs of the piano stool. Crystallographic data, selected bond lengths, and angles are given in Tables S1 and S2.

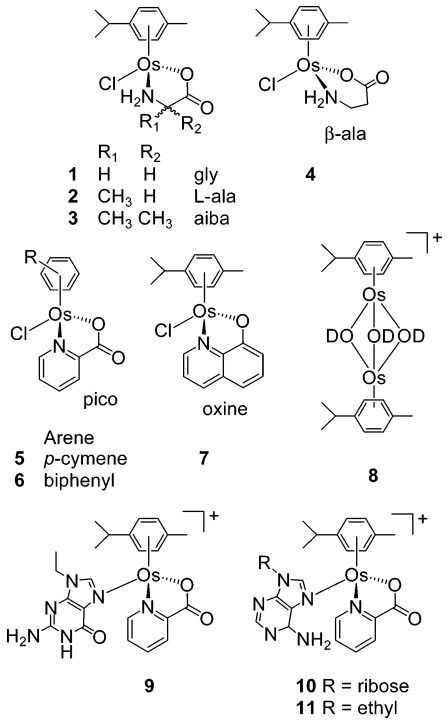

Figure 1. Osmium arene complexes studied in this work.

Independent molecules in the crystal structures of **5** and **7** are linked by short-range interactions between the coordinated chloride and an aromatic ring proton of the chelating ligand (Cl(1)···H(321) 2.81 Å) or *p*-cymene arene (Cl(1)···H(211) 2.69 Å), respectively. Further short-range interactions are present between aromatic ring protons and oxygen atoms of the chelate (Figure S1 and Table S3).

Aqueous Solution Chemistry and pK_a* Determination. Aqueous solutions of the chloro complexes **1**−**6**, directly after sample preparation (<10 min), gave rise to one major and one minor set of ^{1}H NMR peaks, with resolved peaks for each of the four *p*-cymene ring protons, consistent with the presence of stereogenic osmium centers (the L-alanine complex **2** was present as a ca. 1:1 mixture of diastereoisomers). When the pH* values of the solutions were increased from ca. 3 to 10, the major set of NMR peaks gradually shifted to high field (Figure 3A), consistent with assignment to aqua adducts. Plots of the chemical shifts against pH* (Figures 3A and S2) were fitted to the Henderson−Hasselbalch equation and gave rise to pK_a* values between 7.27 and 7.55 for complexes containing both primary amines and carboxylate groups as donors, but lower

(22) Krezel, A.; Bal, W. *J. Inorg. Biochem.* **2004**, *98*, 161−166.
(23) Atkins, P. W. *Physical Chemistry*, 6th ed.; Oxford University Press: Oxford, 1998.
(24) Delpuech, J.-J. *Dynamics of Solutions and Fluid Mixtures by NMR*; John Wiley & Sons: England, 1995.
(25) Skehan, P.; Storeng, R.; Scudiero, D.; Monks, A.; McMahon, J.; Vistica, D.; Warren, J. T.; Bokesch, H.; Kenney, S.; Boyd, M. R. *J. Natl. Cancer Inst.* **1990**, *82*, 1107−1112.

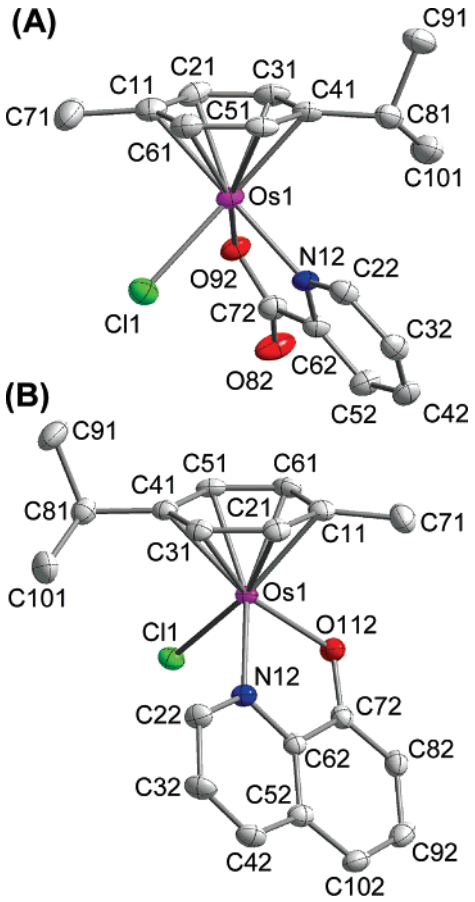

Figure 2. X-ray crystal structures and atom numbering schemes for (A) [(η^6-*p*-cym)Os(pico)Cl] (**5**) and (B) [(η^6-*p*-cym)Os(oxine)Cl] (**7**) (50% probability ellipsoids). H atoms have been omitted for clarity.

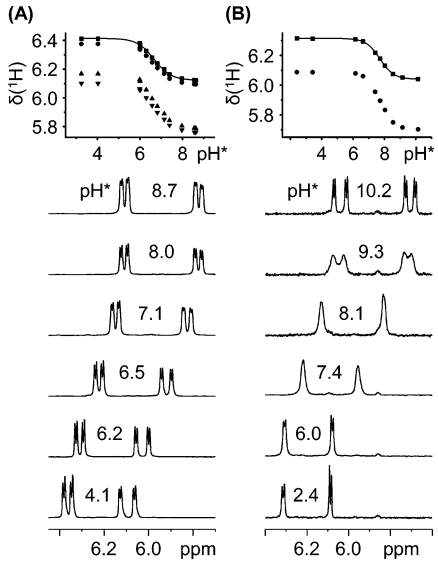

Figure 3. The dependence of the arene region of ^{1}H NMR spectra of (A) [(η^6-*p*-cym)Os(pico)Cl] (**5**) and (B) [(η^6-*p*-cym)Os(oxine)Cl] (**7**) in D_2O on pH*. The plots show fits giving pK_a* values of 6.67 and 7.71 for the aqua complexes **5A** and **7A**, respectively. The four magnetically inequivalent arene ring protons give rise to separate peaks in the spectra of **5A** and exhibit the same pH* dependence. However, the four peaks for **7A** are resolved only at basic pH* and broaden and sharpen into two doublets at acidic pH*, indicative of involvement in a dynamic chemical exchange process.

values of 6.33 and 6.67 for the picolinate complexes (**5** and **6**) which contain pyridine as a tertiary amine donor instead of a primary amine donor (Table 1). The minor sets of peaks for coordinated *p*-cym increased in intensity on addition of NaCl and are assigned to the intact chloro complex (Table S4). During the pH* titration of the β-alaninate complex **4**, new *p*-cym doublets appeared at δ 6.04 and 5.82, with increase in pH*. These peaks have previously been assigned[26] to the hydroxo-bridged dinuclear species, [(η^6-*p*-cym)Os(μ-OD)$_3$Os(η^6-*p*-cym)]$^+$, **8**. After incubation of aqueous solutions of **1**−**4** (2 mM) at 310 K for 24 h (pH* ca. 6.2−6.7), the only changes to the spectra were new peaks for **8** (accounting for 10% of **1**, 6% of **2**, 3% of **3**, and 37% of **4**). NMR spectra of aqueous solutions of the hydroxyquinolate complex **7** contained two doublets assignable to the *p*-cym ring protons of the aqua adduct **7A**, which shifted to high field with increase in pH* (Figure 3B) with an associated pK_a* of 7.71. When the pH* was increased to 8.55, these doublets broadened, and at pH* 10.15, they resolved into four sharp doublets (δ 6.07, 6.01, 5.73, and 5.68; Figure 3B). The NMR spectrum of a solution of **7** in 100 mM NaCl contained four doublets for *p*-cymene ring protons (Table S4) assignable to the intact chloro complex **7**.

Table 1. pK_a* Values for the Deprotonation of the Coordinated D_2O in Complexes **1A**−**7A** and the N1-H of N7-Coordinated Nucleobase in **9** and **11**

complex		pK_a*
[(η^6-*p*-cym)Os(gly)(OD_2)]$^+$	**1A**	7.27
[(η^6-*p*-cym)Os(L-ala)(OD_2)]$^+$	**2A**	7.14
[(η^6-*p*-cym)Os(aiba)(OD_2)]$^+$	**3A**	7.17
[(η^6-*p*-cym)Os(β-ala)(OD_2)]$^+$	**4A**	7.55
[(η^6-*p*-cym)Os(pico)(OD_2)]$^+$	**5A**	6.67
[(η^6-bip)Os(pico)(OD_2)]$^+$	**6A**	6.33
[(η^6-*p*-cym)Os(oxine)(OD_2)]$^+$	**7A**	7.71
[(η^6-*p*-cym)Os(pico)(9-EtG-*N7*)]$^+$	**9**	8.97
[(η^6-*p*-cym)Os(pico)(9-EtA-*N7*)]$^+$	**11**	2.06

Fresh aqueous solutions (5% MeOD-d_4/95% D_2O) containing complexes **1**−**4** at low concentration (50 μM) at 298 K all gave rise to peaks for aqua adducts and for **2** and **4** peaks for hydroxo-bridged dinuclear species **8** as well. After incubation at 310 K for 24 h, compound **8** was present in all the solutions, and for **4**, it was the only species present (Figure S3). Similar solutions of complexes **5** and **6** (50 μM) initially contained a mixture of the intact chloro and aqua complexes, but after incubation, only peaks for the aqua complex were present. Complex **7** was present as the aqua complex both initially and after incubation. It was notable therefore that neither complexes **5**, **6**, nor **7** formed the hydroxo-bridged dinuclear species **8** when incubated at biologically relevant concentrations (50 μM).

^{1}H NMR spectra of **5** in isotonic saline solution (150 mM NaCl), ca. 10 min after sample preparation, contained peaks predominantly for the intact chloro species, together with small peaks assignable to the aqua adducts (<20%). No new peaks appeared in the spectrum after storage at ambient temperature in the dark for 2 months (Figure S4).

The effects of chloride concentrations typical of blood plasma (100 mM), cell cytoplasm (22.7 mM), and cell nucleus (4 mM)[27] on the speciation of **5** in aqueous solution were investigated. ^{1}H NMR spectra of **5** (50 μM) were recorded within 10 min of

(26) Peacock, A. F. A.; Melchart, M.; Deeth, R. J.; Habtemariam, A.; Parsons, S.; Sadler, P. J. *Chem.—Eur. J.* **2006**, 10.1002/chem.200601152.
(27) (a) Martin, R. B. In *Cisplatin Chemistry and Biochemistry of a Leading Anticancer Drug*; Lippert, B., Ed.; Wiley-VCH: Zurich; 1999; pp 183−205. (b) Jennerwein, M.; Andrews, P. A. *Drug Metab. Dispos.* **1995**, *23*, 178−184.

Table 2. Rate Data for the Aquation of Complexes **5** and **6** at Varying Temperatures

compound	*T*/K	k/h^{-1}	$t_{1/2}$/h	E_a/kJ mol^{-1}	$\Delta H^{\ddagger}$/kJ mol^{-1}	$\Delta S^{\ddagger}$/J K^{-1} mol^{-1}
5	278	0.243 ± 0.003	2.85 ± 0.03	91.5 ± 3.0	89.1 ± 3.0	−64.8 ± 10.5
	285	0.697 ± 0.018	0.99 ± 0.03			
	288	1.063 ± 0.035	0.65 ± 0.02			
	298	3.491 ± 0.027	0.20 ± 0.01			
6	278	0.092 ± 0.001	7.51 ± 0.10	93.1 ± 4.4	90.7 ± 4.3	−61.6 ± 15.1
	285	0.211 ± 0.003	3.29 ± 0.04			
	288	0.339 ± 0.008	2.04 ± 0.05			
	298	1.346 ± 0.053	0.52 ± 0.02			

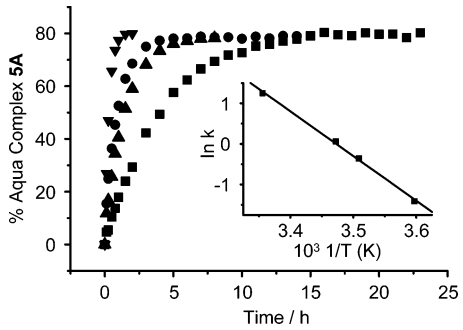

Figure 4. Time dependence for formation of the aqua complex **5A** (based on ^{1}H NMR peak integrals) during hydrolysis of [(η^6-*p*-cym)Os(pico)Cl] (**5**) in acidic (pH* 2) D_2O at 298 K (▼), 288 K (●), 285 K (▲), and 278 K (■). The inset shows an Arrhenius plot the slope of which gives the Arrhenius activation energy E_a of 91.5 kJ mol^{-1}.

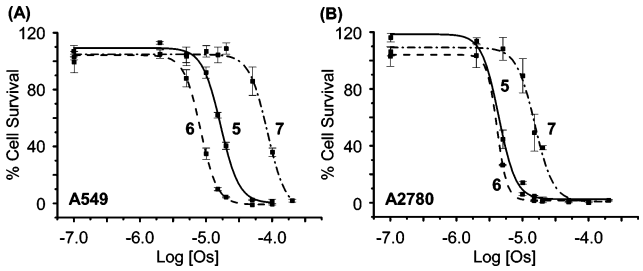

Figure 5. Determination of cancer cell cytotoxicity. Effect of variation in the concentrations of [(η^6-*p*-cym)Os(pico)Cl] (**5**), [(η^6-bip)Os(pico)Cl] (**6**), and [(η^6-*p*-cym)Os(oxine)Cl] (**7**) on the survival of (A) human A549 lung cancer cells and (B) human A2780 ovarian cancer cells, giving the IC_{50} values in Table 3.

Table 3. In Vitro Growth Inhibition of Human A549 Lung and A2780 Ovarian Cancer Cells

compound	IC_{50}/μM A549	IC_{50}/μM A2780
1	>100	>100
2	>100	>100
3	>100	>100
4	>100	>100
5	17	4.5
6	8	4.2
7	60	15.2
Ru-**7**[a]		>100

[a] Ru analogue of **7**, [(η^6-*p*-cym)Ru(oxine)Cl]; see ref 43.

sample preparation and after incubation at 310 K for 24 h. On the basis of ^{1}H NMR peak integrals, complex **5** was found to be present only as the intact chloro complex at 100 mM [Cl] (pH* 7.0), as 45% hydrolyzed complex **5A** at 22.7 mM [Cl] (pH* 7.1) and as 72% **5A** at 4 mM [Cl] (pH* 6.8); see Figure S7 and Table S5.

Kinetics of Hydrolysis. The kinetics of hydrolysis for complexes **1**−**4** and **7** were too fast to measure by NMR. However, we were able to follow the formation of the aqua complexes of **5** and **6** based on integration of ^{1}H NMR peaks in spectra recorded at various time intervals and temperatures. These experiments were carried out at acidic pH* (ca. 2) so that deprotonation of the aqua complex as a secondary reaction did not occur. The hydrolysis data were fitted to pseudo-first-order kinetics (Figures 4 and S5). At 298 K, the half-life for hydrolysis of the *p*-cymene complex **5** was 0.2 h, about 2.5 times shorter than that for the biphenyl complex **6** (Table 2). Arrhenius activation energies (E_a), activation enthalpies ($\Delta H^{\ddagger}$), and activation entropies ($\Delta S^{\ddagger}$) (Figure S6) are listed in Table 2. The large negative $\Delta S^{\ddagger}$ values are notable.

Variable Temperature Dynamic NMR. ^{1}H NMR spectra of aqueous solutions (1 mM, 5% MeOD-d_4/95% D_2O) of complexes **4**, **5**, and **7** (containing predominantly the aqua complexes **4A**, **5A**, and **7A**) at pH* ca. 4 (so as to prevent deprotonation of the coordinated water) were recorded over the temperature range of 275−353 K. At lower temperatures (285 K), four peaks for the *p*-cymene arene protons of the aqua complex **4A** were resolved (doublets at δ 6.27 and 6.22, δ 5.98 and 5.96). These peaks broadened at 323 K (broad peak at δ 6.26, doublet at δ 6.01) but sharpened into two doublets (δ 6.27 and 6.03) at 343 K. The aqua complex **5A** gave four sharp doublets (δ 6.41, 6.38, 6.17, and 6.10) at 293 K, which merged into two broad peaks (δ 6.40 and 6.17) at 353 K. Peaks for the intact chloro complex **5** (accounting for ca. 13% of the species in solution) showed a similar behavior: doublets at δ 6.27, 6.00, and 5.98 at 293 K which merged into broad peaks at δ 6.27 and 6.00 at 353 K. ^{1}H NMR spectra of the aqua complex **7A** contained two *p*-cymene doublets (δ 6.31 and 6.09) at 298 K, one of which broadened on cooling to 283 K (broad peak δ 6.31, doublet δ 6.08) and resolved into broad peaks at δ 6.35 and 6.28, on cooling to 275 K (Figure S8). The rates of the dynamic chemical exchange processes (k_c) which gave rise to these line shape changes, lifetimes of the contributing species (t_c), and the Gibbs free energies ($\Delta G^{\ddagger}$) at the coalescence temperature (T_c) were calculated. These range from $k_c = 47$ s^{-1} at $T_c = 353$ K for **5A**, 57 s^{-1} at 323 K for **4A**, to 102 s^{-1} at 283 K for **7A** (Table S6). ^{1}H NMR spectra of solutions of the intact chloro adducts **5** and **7** in methanol-d_4 were temperature dependent with the four *p*-cymene peaks resolving out at lower temperatures (Figure S8D and E).

Cancer Cell Cytotoxicity. The cytotoxicity of complexes **1**−**7** toward human ovarian A2780 and lung A549 cancer cell lines was investigated. Complexes **1**−**4** were nontoxic up the highest test concentration of 50 μM. The IC_{50} (50% growth inhibitory activity) values are therefore likely to be >100 μM, and with this cutoff value, the complexes are deemed inactive. However, complexes **5**−**7** showed moderate to high activity (Figure 5 and Table 3) with IC_{50} values of 4−60 μM. Notable is the high activity of the biphenyl/picolinate complex **6** against

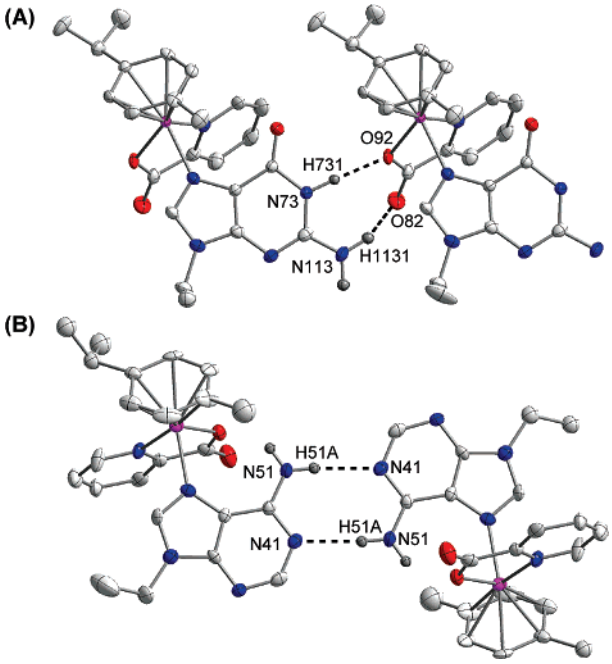

Figure 6. X-ray structures of nucleobase adducts. H-bonded cations in the X-ray crystal structure of (A) $[(\eta^6\text{-}p\text{-cym})Os(pico)(9EtG)]^+$ (**9**), between the oxygen O92/O82 of the chelated pico ligand and N1H (N73H7311) and $C2NH_2$ (N113H1131) of coordinated 9EtG from an adjacent molecule. (B) Metal-modified A:A homo base pairing between C2NH (N51H51A) and N1 (N41) of an adjacent molecule for $[(\eta^6\text{-}p\text{-cym})Os(pico)(9EtA)]^+$ (**11**); 50% probability ellipsoids, remaining H atoms have been omitted for clarity.

both cell lines (IC_{50} 4.2 and 8.0 μM for A2780 and A549 cells, respectively).

Binding to Nucleobases, Possible Target Sites on DNA. The reactions of the cytotoxic complex, $[(\eta^6\text{-}p\text{-cym})Os(pico)\text{-}Cl]$ **5**, with model nucleobases were investigated, as binding to DNA is often associated with the cytotoxic action of metal anticancer drugs.[12,28]

In the ^{1}H NMR spectrum of a solution containing **5** (1 mM) and 1 molar equiv 9-ethylguanine (D_2O, pH* 7.68, 298 K), new peaks assignable to the 9EtG adduct **9** appeared (Figure S9A), with an approximate half-time for reaction, based on peak integrals, of 3.5 h (Figure S9B). ESI-MS studies on this NMR sample gave a major peak at *m*/*z* 627.2, consistent with the presence of $[(\eta^6\text{-}p\text{-cym})Os(pico)(9EtG)]^+$ (**9**, calcd *m*/*z* 627.2). Complex **9** was synthesized, and the X-ray crystal structure of the PF_6 salt confirmed the binding of 9EtG by N7 (Figure S10A). An interesting feature of the structure is the hydrogen bonding between NH and NH_2 of 9EtG and the two O atoms of the chelated picolinate on an adjacent molecule (N(73)H(731)···O(92) 1.91 Å and N(113)H(1131)···O(82) 2.19 Å) giving rise to chains in the crystal (Figure 6A and Table S3).

Binding to N7 of 9EtG in **9** was further confirmed by a pH* titration, monitored by ^{1}H NMR spectroscopy, over the pH* range of 3−12. Peaks assigned to species **9** shifted to high field with increasing pH*, with an associated $pK_a^* = 8.97 \pm 0.02$ (Figure S11A), consistent with N1 deprotonation of N7-bound 9EtG.

Addition of 1 molar equiv of adenosine (Ado) to an aqueous solution of **5** (1 mM, pH* 7.38, 298 K) gave rise to little product in the ^{1}H NMR spectrum after 5 min, but after 24 h, there were

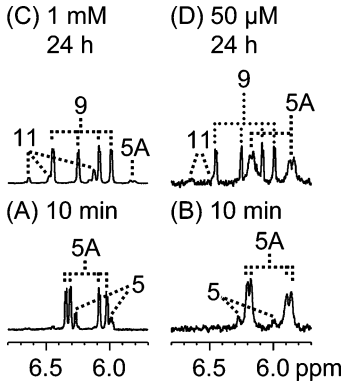

Figure 7. ^{1}H NMR spectra showing the arene CH region for 1:1:1 competition reactions of the aqua adduct **5A** with 9EtG and 9EtA in D_2O at 1 mM and 50 μM. (A) and (B) show the spectra obtained ca. 10 min after sample preparation, and (C) and (D) those obtained after incubation at 310 K for 24 h. **5** and **5A** correspond to the intact chloro and aqua species, respectively, **9** to $[(\eta^6\text{-}p\text{-cym})Os(pico)(9EtG)]^+$ and **11** to $[(\eta^6\text{-}p\text{-cym})Os(pico)(9EtA)]^+$.

two new sets of peaks (38% major species **10** and 21% minor species **10b**). ESI-MS studies on this NMR sample gave peaks at *m*/*z* 448.2 and 715.1, consistent with $\{(\eta^6\text{-}p\text{-cym})Os(pico)\}^+$ ($\{$**5**-Cl$\}^+$, calcd *m*/*z* 448.1) and $[(\eta^6\text{-}p\text{-cym})Os(pico)(Ado)]^+$ (**10**, calcd *m*/*z* 715.2), respectively. Complex **11**, the 9-ethyladenine (9EtA) analogue, was synthesized, and the X-ray crystal structure of the PF_6 salt showed the presence of N7-bound 9EtA (Figure S10B). Hydrogen bonds link independent coplanar 9EtA units in the crystal structure, N(51)H(51A)···N(41) 2.11 Å (Figure 6B). NH_2 of 9EtA and the chelated oxygen of the picolinate ligand are also H-bonded, N(51)H(51B)···O(82) 2.18 Å (Table S3).

The chemical shifts of the H8 and H2 singlets of 9EtA bound to Os in aqueous solutions of **11** shifted to high field with increase in pH* over the range of 1−8, with an associated pK_a^* of 2.06 ± 0.02 (Figure S11B), assignable to N1 protonation of N7-bound 9EtA.

No new peaks appeared in the ^{1}H NMR spectrum of **5** after addition of thymidine (Thy), over a period of 24 h (310 K). However, for cytidine (Cyt), a small set of new peaks appeared accounting for <10% of $\{(\eta^6\text{-}p\text{-cym})Os(pico)\}^+$ present (Figure S12).

The addition of both 1 molar equiv of 9EtG and 1 molar equiv of 9EtA to 1 mM or 50 μM equilibrium solutions of **5** (81 and 90% aqua adduct **5A**, respectively) did not result in any new peaks after ca. 10 min. However, after incubation at 310 K for 24 h, new peaks for **9** and **11** had appeared. On the basis of the peak integrals (Figure 7), the 1 mM solution of **5** contained 6.8% aqua adduct **5A**, 80.7% of the 9EtG adduct **9**, and 12.5% of the 9EtA adduct **11**, a ratio of ca. 0.5:6:1, whereas the 50 μM solution of **5** contained 58.7% aqua adduct **5A**, 32.9% **9**, and 8.4% **11**, a ratio of ca. 7:4:1.

Solutions of the 9EtG adduct **9**, $[(\eta^6\text{-}p\text{-cym})Os(pico)(9EtG)]^+$, in D_2O at varying concentrations (2 mM to 20 μM) were prepared, and their ^{1}H NMR spectra were recorded ca. 10 min after sample preparation and after incubation at 310 K for 24 h, 6 days, and 13 days. No new peaks were present in the spectra recorded after 10 min, but after 24 h, minor new peaks (3% at 2 mM and 12% at 20 μM) appeared, consistent with formation of aqua complex **5A** and free 9EtG; see Figure 8A,C. After incubation of the samples for 6 and 13 days, these peaks

(28) Zhang, C. X.; Lippard, S. J. *Curr. Opin. Chem. Biol.* **2003**, *7*, 481−489.

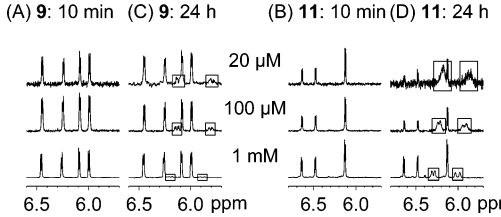

Figure 8. Low-field ^{1}H NMR spectra of 1 mM, 100 μM, and 20 μM solutions of (A) [(η^6-*p*-cym)Os(pico)(9EtG)]$^+$ (**9**) and (B) [(η^6-*p*-cym)Os(pico)(9EtA)]$^+$ (**11**) directly after sample preparation, and (C) and (D) after incubation at 310 K for 24 h. Peaks for the free aqua adduct **5A** are highlighted by boxes. Complex **9** remains mostly intact, whereas complex **11** dissociates almost completely after 24 h (for determination of stability constant, see Figure S13).

increased in intensity. After incubation of the 20 μM solution of **9** for 13 days at 310 K, 40% of the intact complex was still present. Attempts to analyze the data as a simple dissociation were unsuccessful, suggesting that equilibrium had not yet been reached under these conditions. Similarly the stability of 2 mM to 20 μM aqueous solutions of the 9EtA adduct **11**, [(η^6-*p*-cym)Os(pico)(9EtA)]$^+$, was investigated by ^{1}H NMR spectroscopy over a period of 24 h at 310 K. Again, no new peaks were present in the spectra recorded after 10 min; however, after 24 h at 310 K, peaks assignable to free 9EtA and the aqua osmium complex **5A** were present and increased in relative proportion with decrease in Os concentration (Figure 8B,D). An equilibrium binding constant of log *K* 3.95 was obtained from the slope of the plot of [**11**]/[free 9EtG] versus [**5A**], based on peak integration (Figure S13).

Discussion

Our aim in this work was to investigate whether the aqueous chemistry of organometallic osmium(II) arene complexes can be fine-tuned so as to achieve cancer cell cytotoxicity and design potential osmium anticancer agents. Previously, we had found that osmium(II) arene complexes containing en as a N,N-chelating ligand hydrolyze slowly ($t_{1/2}$ = 6.4 h at 298 K and pH* ca. 7), whereas those with β-diketonate O,O-chelating ligands hydrolyze rapidly but are deactivated by chelate ligand loss under biological test conditions.[14] Here we have investigated complexes with mixed N,O-chelating ligands and show that the aqueous reactivity can be fine-tuned even within N,O-chelates by the choice of the types of N- and O-donor groups.

We synthesized chloride complexes **1**−**7** containing primary amine and tertiary pyridine nitrogens as N-donors and carboxylato or aryloxides as O-donors. They were expected to have the familiar half-sandwich, piano-stool structure, and this was verified by X-ray crystal structure determination for two of them, the *p*-cymene/picolinate complex **5** and the *p*-cymene/hydroxyquinolate complex **7**. The structures of Os^{II} arene complexes are often similar to those of their Ru^{II} analogues. Both **7** and its Ru^{II} analogue[16] form almost identical short-range interactions in their crystal structures, and complex **5** is structurally very similar to the related Ru^{II} complex, [(η^6-1,3,5-$C_6Me_3H_3$)Ru(pico)Cl].[15] The Os−Cl bond length in **7** (2.4235(7) Å) is significantly longer than that in **5** (2.4048(13) Å), consistent with the increased charge at the Os^{II} center in **7** and the slower hydrolysis rate of **5**. A similar difference in bond length and hydrolysis rate was noted for Os^{II}/Ru^{II} acetylacetonate and Os^{II}/Ru^{II} ethylenediamine half-sandwich complexes.[14,29] The N,O-chelated complexes studied here are racemates due to the presence of a stereogenic osmium center.

Aqueous Solution Chemistry. Aminoacidate complexes **1**−**4** containing five-membered chelate rings hydrolyzed rapidly ($t_{1/2}$ < min), in agreement with a report for [(η^6-benzene)Os(gly)Cl] ($t_{1/2}$ = 0.6 min at 298 K),[7] a characteristic shared by anionic O,O-chelated Os^{II} and Ru^{II} arene complexes.[14,26,29] Substitution of the primary amine −NH$_2$ donor by the π-acceptor pyridine (complexes **5** and **6**) in N,O-chelated complexes slows down the rate of hydrolysis,[31] and replacement of the arene *p*-cymene (complex **5**) by the more electron-deficient arene biphenyl[7,30] (complex **6**) slows down the rate of hydrolysis even further. The hydroxyquinolate complex (**7**) also hydrolyzes rapidly despite the presence of the π-acceptor pyridine N-donor. This can be attributed to the higher partial charge on the aryloxide O-donor compared to the carboxylate group in **5** where the charge is delocalized over two oxygens. The large negative activation entropies ($\Delta S^{\ddagger}$) obtained for the hydrolysis of **5** and **6** suggest that the mechanism involves an associative pathway. For all of the complexes studied, we observed slow exchange between the chloro and aqua species on the ^{1}H NMR time scale, a characteristic of N,N-chelated complexes, but not O,O-chelated β-diketonate complexes. Hence it appears that N,O-chelated complexes display aqueous chemistry behavior intermediate between that of complexes containing neutral N,N- and anionic O,O-chelating donors, and that within the group of N,O-chelates the choice of N- and O-donor group can have a significant effect.

The acidity of the aqua ligand in the aminoacidate complexes, **1**−**4** (pK_a* 7.14−7.55), is intermediate between that of complexes containing the neutral N,N-chelating ethylenediamine (en), [(η^6-bip)Os(en)(OD$_2$)]$^{2+}$ (pK_a* 6.37), and anionic O,O-chelates such as acetylacetonate (acac), [(η^6-*p*-cym)Os(acac)(OD$_2$)]$^+$ (pK_a* 7.84).[14] Introduction of the π-acceptor pyridine as the N-donor reduces the electron density on the metal, lowering the pK_a* of the coordinated water by 0.6 pK_a* units (Table 1).[32] Due to the unsymmetrical nature of the chelating ligands, the osmium center is chiral in all the complexes studied, as is evident from their aqueous ^{1}H NMR spectra in which all of the protons of the coordinated arene are magnetically inequivalent. This is in contrast to the unsymmetrical O,O-chelated maltolate complexes, for which averaging of proton environments is observed due to a dynamic (ring-opening) process which occurs at the metal center.[26] Complex **5**, for example, in aqueous solution gives four *p*-cymene ^{1}H NMR peaks, each showing the same pH* dependence (Figure 3A). However, complex **7** behaves differently during the pH* titration. At acidic pH*, there are only two sharp doublets in the spectrum; these broaden as the pH* is increased and resolve out into the expected four doublets, one for each arene ring proton, at basic pH* (Figure 3B). This suggests that in acidic

(29) Fernandez, R.; Melchart, M.; Habtemariam, A.; Parsons, S.; Sadler, P. J. *Chem.*−*Eur. J.* **2004**, *10*, 5173−5179.
(30) Dougan, S.; Melchart, M.; Habtemariam, A.; Parsons, S.; Sadler, P. J. *Inorg. Chem.* **2006**, *45*, 10882−10894.
(31) The presence of a π-acceptor ligand can stabilize the transition state in an associative reaction and therefore increase the rate, as observed for square-planar Pt^{II} complexes: Summa, N.; Schiessl, W.; Puchta, R.; van Eikema Hommes, N.; van Eldik, R. *Inorg. Chem.* **2006**, *45*, 2948−2959. If the reaction mechanism for the pseudo-octahedral osmium complexes is associative, H-bonding and steric effects may contribute to the slower rates of hydrolysis.
(32) During the pH* titrations of complexes **1**−**7**, we observed no new independent peaks in the ^{1}H NMR spectra which might be assignable to ring-opened species.

solutions the dynamic process involves rapid chelate ring opening via oxygen atom protonation, which slows down at basic pH*. 8-Hydroxyquinolate is a stronger base (pK_a HQH = 5.0 ± 0.1)[33] than 2-picolinate (pK_a picoH = 1.01)[34] and the other carboxylate N,O-ligands investigated here, suggesting that it would be more readily protonated. This dynamic process was rapid for the maltolate complex [(η^6-*p*-cym)Os(mal)(OD_2)]$^+$, even at basic pH*, which is in keeping with the even higher basicity of maltolate (pK_a malH = 8.62).[26,35] The dynamic process was monitored for D_2O solutions of **4**, **5**, and **7** at various temperatures. The exchange rates imply that ring opening occurs most readily for the oxine complex **7** and least readily for the picolinate complex **5**, which is again consistent with the acidity of the chelated oxygen atom (pK_a of free β-alanine is 3.43).[36] Therefore, the more acidic ligands exhibit enhanced stability with respect to chelate protonation and ring opening, which may also contribute to the higher stability of complexes with respect to formation of the hydroxo-bridged dinuclear species (**8**).

It seems likely that the mechanism of formation of the hydroxo-bridged dinuclear species (**8**) initially involves breakage of the Os−O bond, assisted by protonation, followed by Os−N bond breakage. This does not occur when the chelated ligand contains a pyridine N, despite the ready protonation of the coordinated oxygen in complex **7**. Evidently, the Os−N(pyridine) bond does not break under the conditions studied, preventing formation of the hydroxo-bridged dinuclear species (**8**). Clearly the incorporation of a π-acceptor such as pyridine is crucial for the overall stability of the complex, due to the strengthening of the metal−N bond formed. Complexes containing six-membered aminoacidate chelate rings (complex **4**) show less stability with respect to formation of **8** than their five-membered analogues (complexes **1**−**3**), a trend similar to that found previously for anionic O,O-chelates.[26]

At high chloride concentrations typical of blood plasma (100 mM), complex **5** was present as the less reactive intact chloro species. At the lower chloride concentration of 4 mM (a typical nucleus concentration),[27] the complex is activated by hydrolysis, with 72% present as the reactive aqua species (**5A**). This suggests a possible mode of activation toward DNA binding. In addition, complex **5** was stable in isotonic saline solution when stored in the dark at ambient temperature for 2 months, making aqueous drug formulations feasible.

Complexes containing aminoacidate chelates (**1**−**4**) hydrolyzed rapidly, were unstable with respect to formation of the hydroxo-bridged dinuclear species (**8**), and were inactive toward human ovarian and lung cancer cells. However, complexes **5**−**7** containing a pyridine as the N-donor atom, which were stable at micromolar concentrations and reacted with purine nucleobases, exhibit cytotoxic activity (IC_{50} = 4−60 μM, Table 3). Activity increases with a decrease in the rate of hydrolysis and was greatest for complex **6** which exhibited the slowest kinetics. The rate of hydrolysis of **6** is comparable to the rate of hydrolysis of active ruthenium arene en complexes.[37] IC_{50} values for **6** of 8 and 4.2 μM for the A549 and A2780 cancer cell lines, respectively, are comparable to those of the anticancer drug carboplatin (IC_{50} = 10 and 6 μM for A549 and A2780, respectively).[38,39]

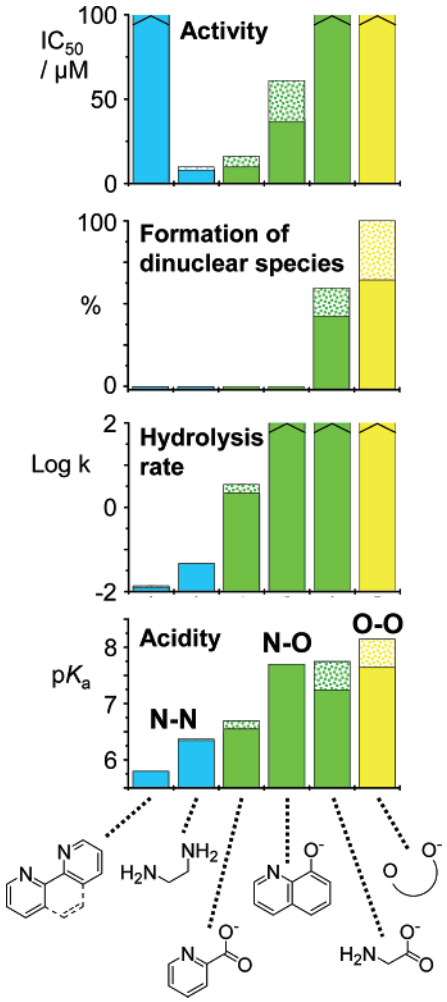

Figure 9. Bar charts illustrating the relationship between cytotoxicity toward human cancer cells, stability with respect to formation of inert hydroxo-bridged dinuclear species, rates of hydrolysis, and acidity of aqua adducts for osmium arene complexes [(η^6-arene)Os(XY)Cl]$^{n+}$ containing different XY = N,N-, N,O-, and O,O-chelating ligands. Shading indicates the range of observed values.

Figure 9 provides an overview of the relationships between cancer cell cytotoxicity, complex stability with respect to formation of hydroxo-bridged dinuclear species, rates of hydrolysis, and acidity of coordinated water. Our work demonstrates how rational chemical design can be applied to osmium arene complexes resulting in specific windows of reactivity, stability, and cancer cell cytotoxicity.

Binding to Nucleobases. Nuclear DNA is often believed to be the major target of metal-based anticancer complexes.[28] Osmium arene complexes, [(η^6-arene)Os(XY)Cl]$^{n+}$, containing a neutral N,N-chelate bind selectively to G-type nucleobases, and those containing an anionic O,O-chelate have similar affinities for both G- and A-type nucleobases.[14,26] The competition reactions carried out with complex **5** show binding to both G and A, but with a strong preference for G. It is notable that,

(33) Irving, H.; Ewart, J. A. D.; Wilson, J. T. *J. Chem. Soc.* **1949**, 2672−2674.
(34) Green, R. W.; Tong, H. K. *J. Am. Chem. Soc.* **1956**, *78*, 4896−4900.
(35) Dutt, N. K.; Rahut, S. *J. Inorg. Nucl. Chem.* **1970**, *32*, 1035−1038.
(36) Včeláková, K.; Zusková, I.; Kennaler, E.; Gaš, B. *Electrophoresis* **2004**, *25*, 309−317.
(37) Wang, F.; Chen, H.; Parsons, S.; Oswald, I. D. H.; Davidson, J. E.; Sadler, P. J. *Chem.—Eur. J.* **2003**, *9*, 5810−5820.
(38) Cui, K.; Wang, L.; Zhu, H.; Gou, S.; Liu, Y. *Bioorg. Med. Chem. Lett.* **2006**, *16*, 2937−2942.
(39) Aird, R. E.; Cummings, J.; Ritchie, A. A.; Muir, M.; Morris, R. E.; Chen, H.; Sadler, P. J.; Jodrell, D. I. *Br. J. Cancer* **2002**, *86*, 1652−1657.

even at micromolar concentrations, >40% of the osmium is bound to purine nucleobases. Intriguingly, the binding constant for 9EtA is only moderate (log *K* 3.95), and equilibrium for dissociation of 9EtA from $[(\eta^6\text{-}p\text{-cym})Os(pico)(9EtA\text{-}N7)]^+$ (**11**) is reached within 24 h of incubation (310 K). In contrast, dissociation of the 9EtG adduct $[(\eta^6\text{-}p\text{-cym})Os(pico)(9EtG\text{-}N7)]^+$ (**9**) at micromolar concentrations occurs relatively slowly, and equilibrium is not reached even after incubation at 310 K for 13 days. Hence, once G adducts (on DNA or RNA) are formed, they are likely to persist. Such kinetic stability may also make G adducts less susceptible to repair compared to A adducts. Binding to the N7 of 9EtG or 9EtA acidifies the N1 proton, which is consistent with metalation at the N7 site.[11,40,41] Little and no binding of $[(\eta^6\text{-}p\text{-cym})Os(pico)Cl]$ to the pyrimidine bases, Cyt and Thy, was observed. The N3 position is sterically crowded in both pyrimidine bases making it an unfavorable binding site, and at physiological pH, N3 of Thy is protonated making it less available for binding (and involved in Watson−Crick H-bonding).

A search of the Cambridge Database revealed no previously reported X-ray crystal structures of osmium complexes containing coordinated guanine or adenine nucleobases. However, the structure of $[Os(9MeHyp)(NH_3)_5]Cl_3\cdot H_2O$ (9MeHyp = 9-methylhypoxanthine), which contains the purine base hypoxanthine (Hyp), has been reported.[42] The X-ray structures of **9** and **11** confirmed the binding of $\{(\eta^6\text{-}p\text{-cym})Os(pico)\}^+$ to the sterically non-hindered N7 site. In solution, a minor product (**10b**; ca. 20%) also formed with adenosine and can be assigned to an N1-bound species. The Os−N7(nucleobase) bond lengths compare well with those reported for $[Os(9MeHyp\text{-}N7)(NH_3)_5]Cl_3\cdot H_2O$ (2.107 Å), $[(\eta^6\text{-}p\text{-cym})Ru(gly)(9EtG\text{-}N7)]PF_6$ (2.136 Å),[43] and $[(\eta^6\text{-benzene})Ru(\text{L-ala})(9EtG\text{-}N7)]Cl$ (2.115(6) and 2.112(7) Å).[44] Intriguingly, the nucleobase functionality lies on opposite sides of the chelate for G and A bases. The exocyclic oxygen of 9EtG is on the N-chelated side of the picolinate ligand, and the NH_2 of 9EtA is on the O-chelated side (as is also the case for related ruthenium complexes),[43,44] both forming favorable short-range interactions with the chelate (O···CH and NH···O, respectively).

Homo base pairing involving $C6NH_2\cdots N1$ ($C51NH_2\cdots N41$) H-bonding is observed between the metal-modified adenine fragments in the X-ray crystal structure of **11** (Figure 6B). This base pairing is of the "extended pairing" type[45] as the N7 position is blocked by the coordinated osmium. Non-Watson−Crick adenine homo base pairing is not unusual and is also present in the X-ray crystal structures of 2′,3′-*O*-anhydroadenosine[46] and tetraaqua-(9-methyladenine) copper(II) sulfate monohydrate.[47,48] Evidence for such pairing has even been found in cytosine-rich DNA at low pH.[49] Such binding to DNA might therefore result in mismatches in the base pairing of adenine. Cisplatin binding to DNA results in 25% of total lesions being ApG intrastrand adducts, and these are 5 times more mutagenic than the more common GpG adducts.[50] Therefore, such interactions resulting from A binding on DNA could contribute to the anticancer activity of complex **5**.

Conclusions

The goal of the present study was to design osmium arene complexes which are cytotoxic toward cancer cells and therefore potential novel anticancer drugs. This has been achieved by employing chemical principles to tune the reactivity, aqueous chemistry, and stability of this class of complexes.

We have found that half-sandwich, piano stool Os^{II} arene complexes of general formula $[(\eta^6\text{-arene})Os(N,O)Cl]$, containing an anionic N,O-chelate, display chemical reactivity intermediate between those of the neutral N,N- and anionic O,O-chelated parent compounds. However, even within this group of N,O-chelates, the choice of the N- and O-donors is crucial. The more acidic the chelated oxygen the less readily ring opening occurs, and the less readily hydroxo-bridged dinuclear species are formed. More critically, the introduction of a π-acceptor such as pyridine (as in complex **5** $[(\eta^6\text{-}p\text{-cym})Os(pico)Cl]$) minimizes chelate ring opening through strengthening the Os−N bond. These factors appear to be crucial in maintaining stability with respect to formation of inert (biologically inactive) hydroxo-bridged dinuclear species which can deactivate osmium arene complexes even at micromolar concentrations and in the presence of saline (0.1 M).[14,26]

Complex **5** shows a strong preference for binding to G bases over A bases, with little or no reaction with pyrimidines. The X-ray crystal structures of the G and A adducts of complex **5** are, as far as we are aware, the first osmium G and A adducts to be reported. Reactivity toward DNA nucleobases, along with the aqueous chemistry and stability (at micromolar concentrations), makes $[(\eta^6\text{-}p\text{-cym})Os(pico)Cl]$ **5**, $[(\eta^6\text{-bip})Os(pico)Cl]$ **6**, and $[(\eta^6\text{-}p\text{-cym})Os(oxine)Cl]$ **7** suitable candidates for further investigation as anticancer agents. These complexes exhibit activity against human A549 lung and A2780 ovarian cancer cells, comparable to that of carboplatin.

Acknowledgment. We thank the EPSRC and The University of Edinburgh (studentship for A.F.A.P.), Rhona E. Aird and Professor Duncan Jodrell (Western General Hospital, Cancer Research UK Centre) for advice and assistance with cell culture, and Dr. Abraha Habtemariam (Edinburgh) and members of EC COST groups D20 and D39 for stimulating discussions.

Supporting Information Available: Details of the crystallographic data (Tables S1−S3, Figures S1 and S10), aqueous chemistry (Tables S4−S6, Figures S2−S8), and nucleobase studies (Figure S9−S13); X-ray crystallographic data in CIF format. This material is available free of charge via the Internet at http://pubs.acs.org.

JA068335P

(40) Sigel, H. *J. Am. Chem. Soc.* **1975**, *97*, 3209−3214.
(41) Inagaki, K.; Kidani, Y. *J. Inorg. Biochem.* **1979**, *11*, 39−47.
(42) Johnson, A.; O'Connell, L. A.; Clarke, M. J. *Inorg. Chim. Acta* **1993**, *210*, 151−157.
(43) Habtemariam, A.; Melchart, M.; Fernández, R.; Parsons, S.; Oswald, I. D. H.; Parkin, A.; Fabbiani, F. P. A.; Davidson, J. E.; Dawson, A.; Aird, R. E.; Jodrell, D. I.; Sadler, P. J. *J. Med. Chem.* **2006**, *49*, 6858−6868.
(44) Sheldrick, W. S.; Heeb, S. *Inorg. Chim. Acta* **1990**, *168*, 93−100.
(45) Robinson, H.; van der Marel, G. A.; van Boom, J. H.; Wang, A. H.-J. *Biochemistry* **1992**, *31*, 10510−10517.
(46) Koole, L. H.; Neidle, S.; Crawford, M. D.; Krayevski, A. A.; Gurskaya, G. V.; Sandstroem, A.; Wu, J. C.; Tong, W.; Chattopadhyaya, J. *J. Org. Chem.* **1991**, *56*, 6884−6892.
(47) Sletten, E.; Thorstensen, B. *Acta Crystallogr., Sect. B* **1974**, *30*, 1961−1966.
(48) Related $Pt^{II}\text{-}G^-\cdots G^-$ and $Pt^{II}\text{−}G^-\cdots G$ homo base pairing between N1 (de)-protonated 9-ethylguanine bases has been observed in the X-ray crystal structure of *cis*-$[Pt(NH_3)_2(9EtG^-)_2]\cdot 4H_2O$ and *cis*-$[Pt(NH_3)_2(9EtG^-)_2]\cdot H9EtG\cdot 7H_2O$, respectively: Schröder, G.; Lippert, B.; Sabat, M.; Lock, C. J. L.; Faggiani, R.; Song, B.; Sigel, H. *J. Chem. Soc., Dalton Trans.* **1995**, 3767−3775.
(49) Lippert, B. *J. Chem. Soc., Dalton Trans.* **1997**, 3971−3976.
(50) Burnouf, D.; Gauthier, C.; Chottard, J. C.; Fuchs, R. P. P. *Proc. Natl. Acad. Sci. U.S.A.* **1990**, *87*, 6087−6091.